Journal of Applied Analysis and Computation
Volume 2, Number 2, May 2012
Website:http://jaac-online.com/
pp. 193–203

ENTROPY COMPUTATION ON THE UNIT DISC OF A MEROMORPHIC MAP

David C. Ni

Abstract We propose a new definition of entropy based on both topological and metric entropy for the meromorphic maps. The entropy is then computed on the unit disc of a meromorphic map, which is called the extended Blaschke function, and is a nonlinear extension of the normalized Lorentz transformation.

We find that the defined entropy is computable and observe several interested results, such as maximal entropy, entropy overshoot due to topological transition, entropy reduction to zero, and scaling invariance in conjunction with parameter space.

Keywords Entropy, dynamical systems, Blaschke, nonlinear Lorentz transformation, scaling.

MSC(2010) 28D20, 30E99, 37A35, 37B40, 37M25.

1. Introduction

The definitions of entropy of a dynamical system, namely, a discrete map or a continuous flow are different from those contemporary ones in physics. Mathematically entropy represents the measures of dynamical complexity as the system evolves with time or in space. For rigor and soundness of the theorems and proofs, we normally explore the maps and flows in conjunction with differentiable structures, such as differentiable manifolds. The key concepts of the efforts include invariant measures on the sets under specific partitions. A common approach for defining a partition is accordingly based on the differentiable structures. For examples, we can read the symbol of $\epsilon \to 0$, namely, number of partition becoming infinite in the definitions of topological entropy, Kotak's entropy, Brin-Kotak entropy, Romagnoli's entropy, Ornstein-Weiss type entropy, Modified Bowen entropy, Newhouse's local entropy, Modified Misiurewicz's entropy, etc. A comprehensive review and update are in [4] and the references therein.

From the perspectives of the recent efforts toward bridging the definitions between mathematics and physics [3], and the limitation of numerical analysis, we face new challenges. The first challenge is that we need to handle singularities of non-smooth structures in the physical world, and secondly the computing hardware can only provide finite resolutions. In 2002, Milnor raised several questions in an article entitled "Is Entropy Effectively Computable" [5] as follows:

- Is there a maximum error for a given resolution for either topological or metric entropy?

Email address:davidcni@yahoo.com
Research, Direxion Technology, Taipei, Taiwan, China

- Is there an effective procedure to carry out the computation in a reasonable time?
- Topological entropy does not always depend continuously on parameters.
- Are both upper and lower bound of the defined entropy effectively computable?

The topological entropy of a map F can be described as the *supremum* over all finite F-invariant sets in conjunction with a partition of a bounded region containing a probability measure which is invariant under F [1]. The metric or measure-theoretic entropy introduced by Kolmogorov and Sinai in 1959 can be described as the *supremum* in conjunction with a set of partitions of a phase space, where the orbits stepping forward with a probability measure. Other definitions also face the same questions raised by Milnor. Some ideas, such as variational principle, were introduced to develop structures and computing procedures for answering these questions. However, general and solid examples for the structures with singularities are still under intensive researches.

In this paper, we construct a meromorphic map, which is a nonlinear extension of the normalized Lorentz transformation and define a new version of entropy based on the concepts of ratio of preimage of divergent and convergent partitions, namely, Julia sets and Fatou sets. This approach allows us to simplify the procedure of computing entropy in the momentum space instead of computing with time and in phase space.

2. Construction of Maps

2.1. Maps

Given two inertial frames with different velocities, u and v, the observed velocity, u, from v-frame is as follows:

$$u' = \frac{u - v}{1 - \frac{vu}{c^2}}. \tag{2.1}$$

We set $c^2 = 1$ and then multiply a phase connection, $exp(i\phi(u))$, to the normalized complex form of the equation (2.1) based on gauge transformation as follows:

$$\frac{u'}{u} = \frac{1}{u} exp(i\phi(u)) \frac{u - v}{1 - uv}. \tag{2.2}$$

We further define a generalized complex function in conjunction with phase connection, $\exp(i\phi(u))$, as follows:

$$f_B(z, m) = z^{-1} \prod_m C_i, \tag{2.3}$$

and C_i has the following forms:

$$C_i = exp(g_i(z)) \frac{a_i - z}{1 - \bar{a}_i z}, \tag{2.4}$$

where z is a complex variable representing the velocity u, a_i is a parameter representing velocity v, $\bar{a}_i$ is the complex conjugate of a complex number a_i, and m is

an integer representing the functional order. The term $g_i(z)$ is a function assigned to $\sum^p 2p\pi iz$ with p as an integer.

The function $f_B(z, m)$ is called an extended Blaschke function (EBF) [2]. The extended Blaschke equation (EBE) is defined as follows:

$$f_B(z, m) - z = 0. \tag{2.5}$$

For $m = 1$ case, we have the normalized Lorentz transformation. For $m > 1$ cases, we have nonlinear extension of Lorentz transformation. The convergent sets of EBF represent the stable sets of normalized momentum of the particles interacting nonlinearly with others in an ensemble.

2.2. Original and Mapped Domains

A domain can be the entire complex plane, C_∞, or a set of complex numbers, such as $z = x + yi$, with $(x^2 + y^2)^{1/2} \leq R$ and R is a real number. For solving the EBE, a function f will be iterated as:

$$f^n(z) = f \circ f^{n-1}, \tag{2.6}$$

where n is a positive integer indicating the number of iteration. The function operates on a domain, which is called the original domain. The sets of $f^n(z)$ is called the mapped domain. In the figures of this paper, the regions in black color represent Fatou sets containing the convergent points of the concerned functions or equations and the white (i.e., blank) regions correspond to Julia sets, the complementary sets of Fatou sets on C_∞. The original domain is analogical to the preimage of the holomorphic maps.

2.3. Parameter Space

In order to characterize and to classify the original and the mapped domains, we define a set of parameters, which is the parameter space, for specifying the concerned domains. The parameter space includes five parameters: 1) z, 2) a, 3) $exp(g_i(z))$, 4) m, and 5) $iteration$. In the context of this paper, we use the set $\{z, a, exp(g_i(z)), m, iteration\}$ to represent the parameter space. For example, $\{a\}$, is one of the subsets of the parameter space.

2.4. Conformal Mapping and Fractals

On the complex plane, the convergent domains of the functions form fractal patterns with limited-layered structures, which demonstrate skip-symmetry, symmetry broken, chaos, and degeneracy in conjunction with parameter space [6].

Figure 1(a) and 1(b) show the original and the mapped domains of $f_B(z, 11)$ respectively. This Figure shows a conformal mapping from the original domain to the mapped domain. Figure 2 shows two types of the fractal patterns of the original domains. These patterns are plotted on the different scales. In order to show the figures more observable, we intend to reverse the color tone of the Fatou and Julia sets, namely, the sets in the black color are the Julia sets in the Figure 2.

Conformal mapping and fractal patterns directly verify that the numerical results are not generated by the embedded algorithms in the computer architecture.

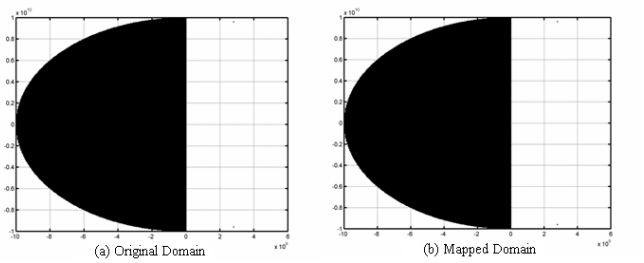

Figure 1. (a) Original Domain and (b) Mapped domain of $f_B(z, 11)$

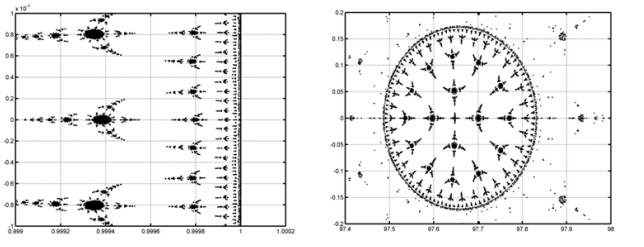

Figure 2. Fractal Patterns of the Original Domains

2.5. Layered Ring Structure

The Fatou sets of the original domains form ring structures with the fractal patterns. The smaller rings are inside the larger rings. For $m > 2$ cases, there exist five layers of rings as shown in Figure 3. The ring on scale of 10^{-2}, Fig. 3(b), is topologically similar to that on scale of 10^5 as shown in Fig. 3(e). We called this observation as skip symmetry. The value of a will determine the size and number of layers of the rings [5].

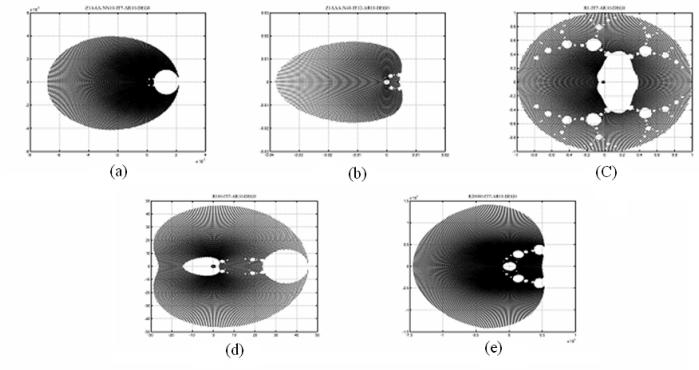

Figure 3. Five layers of ring structure of Fatou sets on different scales for $a = 0.1$ and $m = 3$

3. Topological Transition of Parameter-dependent Domains

The parameters in the parameter space determine the topological structures of the domains. In this section, we examine two cases related to the parameter $\{a\}$.

3.1. Nonlinear to Linear Degeneracy

Figure 4 shows the Fatou sets of the original domains with different values of the parameters $\{a, m\}$. Figure 4(a) through (d) show that the Fatou sets are topologically different from $f_B(z, 1)$ to $f_B(z, 4)$ when $a = 0.1$. When the value of $\{a\}$ increases from 0.1 to 0.8, the Fatou sets show topologically analogy with minor variations from $f_B(z, 1)$ to $f_B(z, 4)$, as shown in Fig. 4(e) through 4(h), or even at higher values of $\{m\}$. We call this observation as nonlinear-to-linear degeneracy [7]. As the degeneracy continues to evolve, the layered-ring structure for all $m > 1$

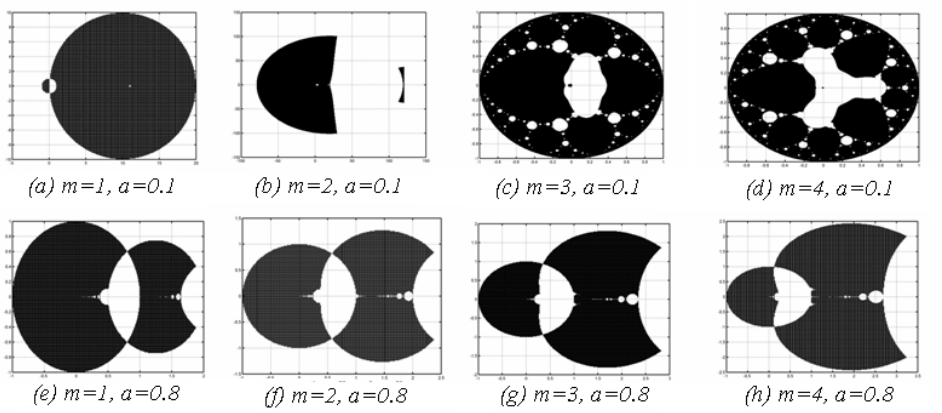

Figure 4. Original Domains of $f_B(z, 1)$, $f_B(z, 2)$, $f_B(z, 3)$, and $f_B(z, 4)$ with values of $\{a\}$ at 0.1 and 0.8 respectively

domains, such as figures shown in Fig. 3, will collapse into the Fatou sets, which are topologically analogical to those of $f_B(z, 1)$ case.

3.2. Continuous to Discrete Transition

As the value of $\{a\}$ is further approaching to unity, we observe the continuous and connected Fatou sets transform into discrete Cantor-like sets. Figure 5(a) shows that the sets in Fig. 4(h) further transform into a unit disc with the shrinking fractal patterns on the scale of 10^{-7} at the vicinity of $z = 1$. Figure 5(b) shows the continuous and connected Fatou sets transform into Cantor-like sets when $1 - a \sim 10^{-17}$. This interesting property may potentially bridge the theories of relativity and quantum mechanics [7] .

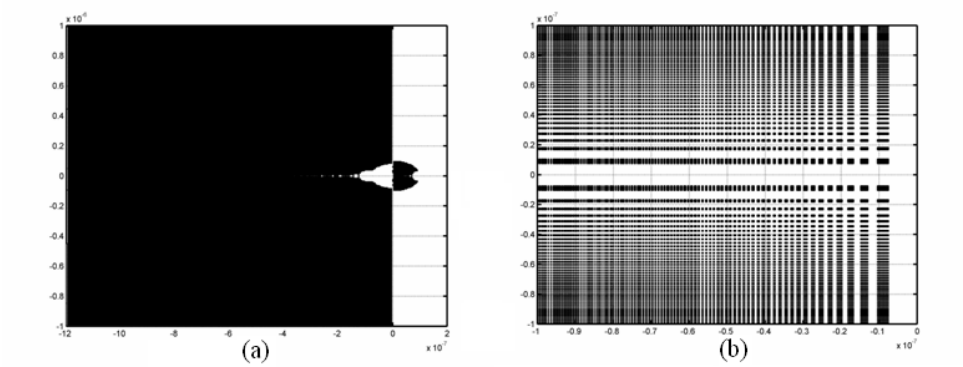

Figure 5. Fractal pattern (a) transforms to discrete Cantor-like sets (b) of the original domains on the scale 10^{-7} near $z = 1$ on Complex plane

4. Entropy Definition

From the computation perspective, we define a new version of entropy in order to explore Milnors questions.

Definition 4.1. Let X be a subset of C_∞, a topological partition of X is dividing X into a group of subsets such that the individual subset has no intersection with one another.

Definition 4.2. Let $f : X \to Y$ be a map on C_∞ with X and Y are subsets of C_∞. If X_j is the union of Julia sets in X, then the normalized entropy of f, denoted by $h_{norm}(f)$, is defined to be

$$0 \leq h_{norm}(f) = P(X_j)/P(X) \leq 1, \tag{4.1}$$

where $P(X_j)$ and $P(X)$ are the σ-algebra measures on a given topological partition of X_j and X, respectively.

We propose these definitions with the assumption that there are conditionally invariant properties between $P(X)$ and $P(Y)$ of the meromorphic map in this study.

5. Entropy Computation

Since the layered ring structure of the original domains of EBF(f_B) demonstrates a property of parameter-dependent area growth, we limit the computation of the normalized entropy on the unit disc, as shown in Fig. 4(c) and 4(d). Further exploration on the entropy related to area growth will be addressed in a future publication. To compute the entropy, we firstly analyze the sensitivity of entropy values to the topological partition and parameter $\{iteration\}$. Then we continue to analyze the dependency of entropy values on the parameters $\{a\}$ and $\{m\}$.

5.1. Entropy vs. Topological Partition

Figure 6 shows the computed entropy values with different topological partitions in conjunction with three parameter $\{a\}$ values. The unit disc is covered by the squares

with side length at 0.01, 0.005, 0.002, and 0.001 respectively. The computed entropy values show that only small variations in the range of 0.2% for the four different topological partitions.

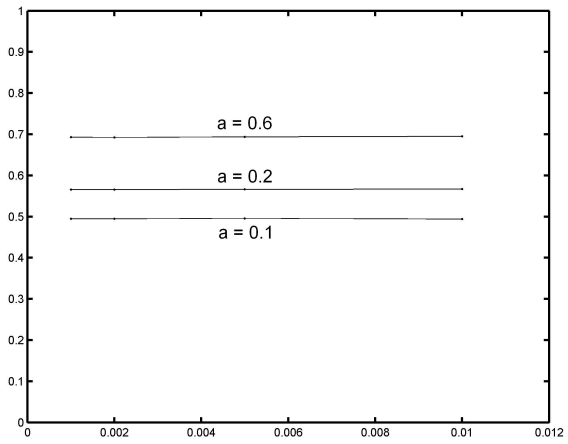

Figure 6. Normalized entropy vs. 4 topological partitions at 3 different $\{a\}$ values

5.2. Entropy vs. Iteration

Figure 7 shows the computed entropy values with different iterations in conjunction with three parameter $\{a\}$ values of a given partition. The computed entropy values show only small variations in the range of 0.5% when the *iteration* ≥ 20.

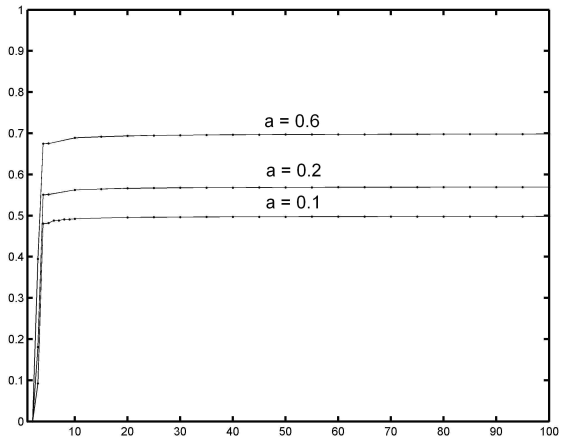

Figure 7. Normalized entropy vs. iteration

5.3. Entropy vs. Functional Order

Figure 8 shows the computed normalized entropy values versus logarithm of base 10 of the functional orders with $a = 0.5$. There are three regions: linear, overshoot, and nonlinear regions and two characteristic functional orders: Maximal Entropy and Stability Edge. The latter order shows the entropy value suddenly drops to a value close to zero, namely, the Julia sets diminish.

In the linear region, the topological patterns of the Fatou sets are shown as in Fig. 4(a). In the overshoot region, the Fatou sets diminish. This region is directly related to the linear-to-nonlinear degeneracy as described in Section 3.1. In the nonlinear region, the Julia sets will grow to a peak value at specific functional order depending of parameter $\{a\}$. This peak value is called the Maximal Entropy. The normalized entropy will then decline as the functional order increases and suddenly drops to a value close to zero at a second functional order indicated as Stability Edge in Fig. 8. Beyond the Stability Edge, the Julia sets diminish.

Figure 9 shows the computed entropy values versus logarithm of base 10 of the functional orders with $a = 0.1, 0.5, 0.9, 0.99, 0.999$, and 1, respectively. In the figure, we observe the following interested properties: a) for all individual $\{a\}$ value except $a = 1$, there exists one maximal value and one stability edge excluding the overshoot region, b) there exists an invariant scaling factor of the functional order between maximal entropy and stability edge. c) for $a = 1$ case, the entropy values are computed after the continuous-to-discrete transition occurs as described in Section 3.2.

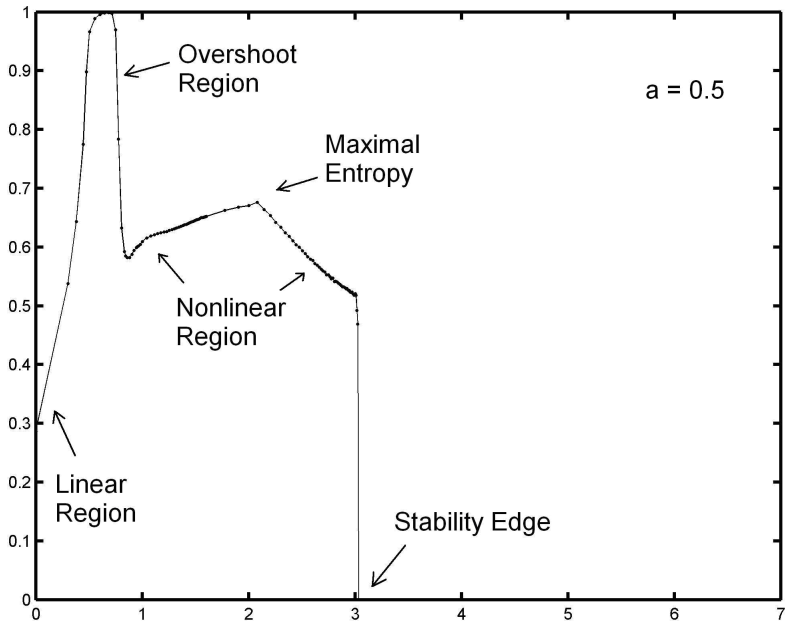

Figure 8. Normalized entropy vs. log_{10}(functional order)

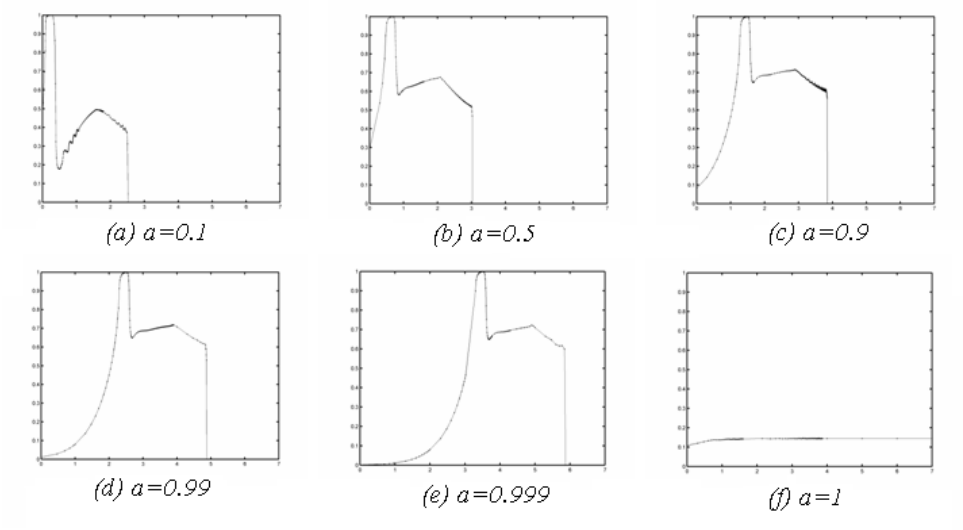

Figure 9. Normalized entropy values for different a vs. log_{10}(functional order)

Figure 10 shows that for individual $\{a\}$ parameter, the ratio of the functional orders between stability-edge and maximal entropy is a constant, which is approximately ~ 8.75. This observation induces the following definition and proposition in the context of computation of the proposed normalized entropy.

Definition 5.1. Let $f : X \to Y$ be a map on C_∞ with X and Y are subsets of C_∞. A scaling invariance under f on a subset of X is defined to be a property of f, which is independent of a subset of the parameter space of f.

Proposition 5.1. *Let $f_B(z, m) : XY$ on C_∞ with X and Y are subsets of C_∞. The ratio of the functional order between the upper bound and onset of lower bound of the normalized entropy of $f_B(z, m)$,i.e., $h_{norm}(f)$, is scaling invariant on the unit disc.*

6. Remarks

This paper proposes a new version of entropy definition based on both topological and metric entropy. We define the normalized entropy as the ratio of topological partition of Julia sets, where the map divergent, over the topological partition of total bounded region, which is the unit disc in this paper. Based on the definition, we perform computation on the entropy and find this special case:

- For a reasonable resolution based on the topological partition, we are able to obtain a known computing error for the computed values.
- For a reasonable iteration, such as $iteration = 20$, in this study, we are able to obtain the entropy values with a definite accuracy in a reasonable computing time.
- There are parameter-dependant transitions, such as the continuous-to-discrete transition, wherein the normalized entropy does not depend continuously on

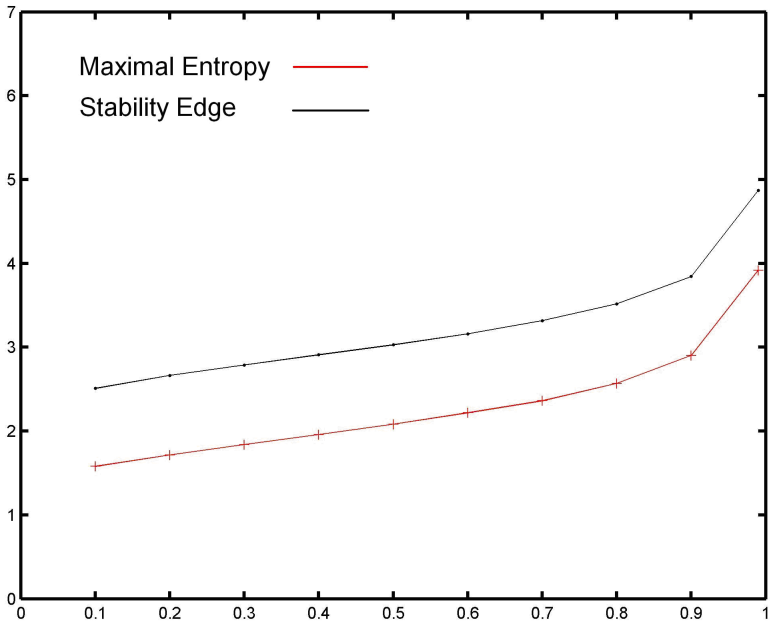

Figure 10. Log_{10}(functional orders) vs. parameter $\{a\}$ values for maximal-entropy and stability edge

parameters.

- We are able to compute both upper and lower bounds of the normalized entropy.

In addition, we have potential to bridging the entropy definitions between mathematics and physics since the stable sets of normalized momentum space representing the allowable momentum values in a normalized ensemble. In this study, we can argue that the max-entropy, where the system demonstrates highest complexity, corresponding to the definition of minimal entropy in physics and the minimal entropy at stability edge, where the system becomes stable and randomized, corresponding to the maximal entropy in physics.

7. Acknowledgement

The author appreciates the opportunity to participate the conference entitled "Frontiers of Complex dynamics" in Banff Center, Alberta, Canada, Feb. 21-25, 2011 and would like to dedicate this paper to John Milnors 80^{th} birthday.

References

[1] R. Adler, A. Konheim and M. McAndrew, *Topological entropy*, Trans. Amer. Math. Soc., 114 (1965), 309-319.

[2] W. Blaschke, *Eine Erweiterung des Satzes von Vitali über Folgen analytischer Funktionen*, Berichte Math.-Phys. Kl., Sächs. Gesell. der Wiss. Leipzig , 67 (1915), 194-200.

[3] Conference proceedings of Frontiers of Complex dynamics (in preparation), Banff Center, Alberta, Canada, Feb. 2011.

[4] T. Donarowicz, *Entropy in Dynamical Systems*, Cambridge University Press, May 2011 (ISBN: 9780521888851).

[5] J. Milnor, *Is Entropy Effectively Computable*, Jan. 2002.

[6] D. C. Ni and C. H. Chin, *Classification on Herman Rings of Extended Blaschke Equations*, Differential Equations and Control processes, 2 (2010), http://http://www.math.spbu.ru/diffjournal/EN/numbers/2010.2/issue.html.

[7] D. C. Ni, *Numerical Studies of Lorentz Transformation*, presented in 7th EAS-IAM, Kitakyushu, Japan, June, 2011, 27-29.